HIGH RESOLUTION ELECTRONIC SPECTROSCOPY OF NITROGEN-CONTAINING MOLECULES IN THE GAS PHASE: 26DAP AND PYRBN

by

Casey Lynn Clements

B.S. Chemistry, Grove City College, 2007

Submitted to the Graduate Faculty of the School of Arts and Sciences

in partial fulfillment

of the requirements for the degree of

Master of Science in Chemistry

University of Pittsburgh

2010

UNIVERSITY OF PITTSBURGH

School of Arts and Sciences

This thesis was presented

by

Casey Clements

It was presented on

November 19, 2010

and approved by

Dr. David Waldeck, Professor, Chemistry

Dr. Lillian Chong, Assistant Professor, Chemistry

Thesis Director: Dr. David Pratt, Professor, Chemistry

HIGH RESOLUTION ELECTRONIC SPECTROSCOPY OF NITROGEN-CONTAINING MOLECULES IN THE GAS PHASE: 26DAP AND PYRBN

Casey Clements, M.S.

University of Pittsburgh, 2010

High resolution gas phase electronic spectra were recorded for 2,6-diaminopyridine (26DAP) and pyrrolidinobenzonitrile (PYRBN). A comparison of the electronic properties of the nitrogen-containing rings aniline, 2-aminopyridine, and 2,6-diaminopyridine (26DAP) shows that the potential energy surface of the molecule is significantly affected as more nitrogen atoms are added to the system. High resolution, rotationally resolved spectra of four vibrational bands in the $S_1 - S_0$ electronic transition of 26DAP were obtained in order to explain these changes. The zigzagging inertial defects point to a double minimum excited state potential energy surface along the coupled amino group inversion vibrational mode, which becomes a four-fold well (and barrier) problem when the existence of two nearly degenerate isomers is taken into account. Assuming that the molecules are in the lower energy, opposite-side configuration, ab initio calculations were performed using the MP2/6-31G** level of theory to create a potential energy surface modeling the simultaneous antisymmetric NH_2-inversion mode. The calculated potential energy surface shows a ground electronic state barrier to simultaneous NH_2 inversion of ~ 220 cm^{-1}, and a fit to experimental vibrational energy level spacings and relative intensities

produces an excited electronic state barrier of ~ 400 cm^{-1}. The ground state barrier is less than that in aniline, but the excited state barrier is larger.

Pyrrolidinobenzonitrile (PYRBN), a derivative of DMABN, has been examined here using high resolution fluorescence excitation spectroscopy in the presence of an electric field varying from 0 – 846 V/cm. The b-type fluorescence band reveals that the transition moment is along the short, in plane axis of the molecule. Upon excitation the inertial defect remains unchanged, which suggests that the molecule's planarity remains constant. The dipole moment is found to increase from 8.06 to 10.45 D upon electronic excitation. This analysis of PYRBN leads to many interesting comparisons to 1PP including their transition moments, dipole moments, and inertial defects.

FOREWORD

I would like to thank my advisor Dr. David Pratt for patience and guidance, and my fellow group members for support and helpful conversations. I would also like to thank Dr. Ken Jordan, Dr. Wissam Al-Saidi, Dr. Daniel Schofield, and Xiaoge Su for their assistance with the theoretical calculations. Funding from NSF Grant # CHE-0911117 also is acknowledged.

TABLE OF CONTENTS

LIST OF TABLES

LIST OF FIGURES

LIST OF SCHEMES

LIST OF EQUATIONS

1.0 INTRODUCTION

Studying biomolecules in the gas phase has the potential to provide insight into areas such as protein folding, nucleic acid base pairing, dipole determination, and electronic structure identification. This work seeks a molecular-level understanding of important biological processes. In particular, this work focuses on the study of nitrogen containing rings and their electronic properties. Nitrogen-containing rings play important roles in many diverse biological systems, from DNA base pairs to the amino acids that make up peptides. The more that can be learned about these nitrogen containing ring systems, the better able scientists will be to understand the biological systems that they compose. Due to the lone pair of electrons on the ring nitrogen, nitrogen containing rings have the potential for electronic properties that are very different from pure carbon rings.

The study of gas phase high resolution electronic spectra reveals rotational constants which can give insight into the structure of a molecule and a transition moment that reveals how the electronic distribution in a molecule is changed by the absorption of light. In order to obtain rotational constants and information about the electronic structure of the molecule, a spectrum needs to be fit. The JB95 spectral fitting program was developed by previous group members and is used to fit the spectra obtained in the high resolution laboratory. The program requires an initial estimate of ground and excited state rotational constants, which are found using Gaussian calculations. From those initial rotational constants, the rigid-rotor Hamiltonian ($H_r = A\ J_a^2 + B\ J_b^2 + C\ J_c^2$) is used to simulate a spectrum. A different H_r is needed for each electronic state, owing to the fact that different states have different rotational constants. The

calculated spectral transitions are manually assigned to experimental transitions and then values of rotational constants and inertial defects are found using a least-squares fitting procedure. This process of simulation, assigning transitions, and running a least-squares fit is continued until a low value for the observed minus calculated (OMC) standard deviation is reached.

In Chapter 2, a study was performed to determine the effect of adding additional nitrogen atoms to the system. Specifically, this work will present a comparison of aniline, 2-aminopyridine (2AP), and 2,6-diaminopyridine (26DAP). Aniline and 2AP have been studied in high resolution by previous group members, and this work adds the analysis of 26DAP. High resolution, rotationally resolved spectra of four vibrational bands in the $S_1 - S_0$ electronic transition of 26DAP were obtained. The zigzagging inertial defects point to a double minimum excited state potential energy surface along the coupled amino group inversion vibrational mode, which becomes a four-fold well (and barrier) problem when the existence of two nearly degenerate isomers is taken into account. The calculated potential energy surface shows a ground electronic state barrier to simultaneous NH_2 inversion of ~ 220 cm^{-1}, and a fit to experimental vibrational energy level spacings and relative intensities produces an excited electronic state barrier of ~ 400 cm^{-1}. The ground state barrier is less than that in aniline, but the excited state barrier is larger.

Chapter 3 presents a study of the change in dipole moment of pyrrolidinobenzonitrile (PYRBN) upon electronic excitation. Electronic excitation of a molecule related to PYRBN, 1-phenylpyrrole, to its first excited state, results in a reversal of the direction of its permanent

electric dipole moment.[1] This work seeks to understand if PYRBN exhibits the same behavior. 1PP and PYRBN are of interest because they are capable of undergoing twisted intermolecular charge transfer (TICT) upon electronic excitation. TICT molecules are capable of displaying two types of fluorescence, including normal b-type fluorescence that can be assigned to an S_1 - S_0 transition from a locally excited state, and in solution an a-type fluorescence that is believed to be from a TICT state stabilized by polar solvent.

In this work, high resolution gas phase spectra of PYRBN were recorded at varying external electric field strengths. This study has confirmed that the origin band of PYRBN involves an L_b state (using Platt's notation) and that no change in planarity occurs upon excitation to that state, as seen by the unchanged inertial defect in the 100% b-type band. The dipole moment increases in magnitude, but does not change direction upon electronic excitation, which is in contrast to 1PP.

1.1 REFERENCES

1. J. A. Thomas, J. W. Young, A. J. Fleisher, L. Alverez-Valtierra, and D. W. Pratt, J. Phys. Chem. Lett. **2010**, *1*, 2017-2019.

2.0 ROTATIONALLY RESOLVED $S_1 - S_0$ ELECTRONIC SPECTRA OF 2,6-DIAMINOPYRIDINE: A FOUR-FOLD BARRIER PROBLEM

2.1 ABSTRACT

A comparison of the electronic properties of the nitrogen-containing rings aniline, 2-aminopyridine, and 2,6-diaminopyridine (26DAP) shows that the potential energy surface of the molecule is significantly affected as more nitrogen atoms are added to the system. High resolution, rotationally resolved spectra of four vibrational bands in the $S_1 - S_0$ electronic transition of 26DAP were obtained in order to explain these changes. The zigzagging inertial defects point to a double minimum excited state potential energy surface along the coupled amino group inversion vibrational mode, which becomes a four-fold well (and barrier) problem when the existence of two nearly degenerate isomers is taken into account. Assuming that the molecules are in the lower energy, opposite-side configuration, *ab initio* calculations were performed using the MP2/6-31G** level of theory to create a potential energy surface modeling the simultaneous antisymmetric NH_2-inversion mode. The calculated potential energy surface shows a ground electronic state barrier to simultaneous NH_2 inversion of ~ 220 cm^{-1}, and a fit to experimental vibrational energy level spacings and relative intensities produces an excited electronic state barrier of ~ 400 cm^{-1}. The ground state barrier is less than that in aniline, but the excited state barrier is larger.

2.2 INTRODUCTION

Studying biomolecules in the gas phase has the potential to provide insight into areas as diverse as protein folding, nucleic acid base pairing, light-induced changes in charge distributions, and electronic structure identifications. Nitrogen-containing molecules play important roles in many different biological systems, from DNA base pairs to the amino acids that make up peptides. The more that can be learned about these molecules, the better equipped scientists will be to understand the function of biological systems that are constructed from them.

This report will focus on the properties of nitrogen-containing aromatic rings and their electronic structure. Owing to the lone pair of electrons on the nitrogen atom, rings containing them have the potential to exhibit properties that are very different from molecules containing pure carbon rings. In order to study the effect of adding additional nitrogen atoms to the system, we present here a comparison of the S_1-S_0 electronic spectra of aniline, 2-aminopyridine (2AP), and 2,6-diaminopyridine (26DAP). Aniline[1] and 2AP[2] have been studied previously at both low and high resolution; this work adds the analysis of 26DAP and its comparison to aniline and 2AP. 26DAP is of interest to the scientific community as a model molecule for studying hydrogen-bonded base pairs.[3, 4] We find that 26DAP is a very different molecule from the parent species aniline and its fellow derivative 2AP in both its ground and electronically excited states.

2.3 EXPERIMENTAL

26DAP was purchased from Aldrich and used without further purification. Low resolution, or vibrationally resolved, electronic spectra were recorded in our low resolution laser laboratory. The 26DAP sample was heated to ~ 90 °C and, using a ~ 0.5 ktorr helium carrier gas, expanded into a vacuum chamber (10^{-5} torr) through a 1 mm pulsed valve (General Valve Series 9) operating at 10 Hz. That expansion was crossed 2 cm downstream of the nozzle with the externally frequency doubled (KDP crystal) output of a dye laser (Quanta Ray PDL-1) using Kiton Red laser dye, pumped by the second harmonic of a Nd^{3+}:YAG laser (Quanta Ray DCR-1A), also operating at 10 Hz. The resulting fluorescence was collected by a photomultiplier tube (PMT, EMI 98139B), processed by a boxcar integrator (Stanford Research Systems), normalized with respect to laser power, and recorded by a data acquisition computer.

Rotationally resolved electronic spectra were observed using the CW molecular beam spectrometer described in detail elsewhere.[5] Briefly, approximately 1 g of 26DAP was heated in a quartz reservoir to around 120 °C (which is slightly below its melting point), seeded into argon backing gas at ~500 torr and expanded through a ~ 200 μm nozzle. The expansion was skimmed 2 cm downstream by a 1 mm skimmer and probed with the laser 15 cm downstream from the nozzle. The excitation source was an Ar^{+}-pumped CW, single-frequency tunable ring dye laser externally doubled by a Spectra-Physics Wavetrain using a 600 nm BBO crystal, yielding ~ 100 μW of power in the UV. The single rovibronic level linewidths were minimized by aligning the molecular beam and laser beam at right angles. The fluorescence was collected using spatially selective optics and detected by a PMT (EMI 9813QB). The data collected were processed using jba95 data acquisition software.[6] Absolute frequencies were determined by

comparison to the iodine absorption spectrum[7] which was simultaneously recorded, providing an absolute frequency accuracy of +/- 30 MHz. Relative frequencies were determined using frequency markers that were created by passing a small portion of the fundamental through a stabilized etalon with a free spectral range of 299.7520 ± 0.0005 MHz and are accurate to 1 MHz or less.

2.4 RESULTS

Figure 2.1 shows the vibrationally resolved fluorescence excitation spectrum of 26DAP. The origin band of the $S_1 - S_0$ transition is located at 32464.9 cm^{-1}. Three vibronic bands of moderate intensity are located within 520 cm^{-1} of the electronic origin band, at frequencies of +164.8, 314.0, and 516.8 cm^{-1} relative to the origin. Notably, while these bands have relative intensities that suggest motion along a single vibrational coordinate, in accord with the Franck-Condon principle, their spacings (~ 165, ~ 150, and ~ 204 cm^{-1}) are not harmonic. Additionally, the low resolution spectrum also exhibits two lower intensity doublets in the vicinity of the origin band, in expansions containing helium. Their absence in argon expansions leads to the conclusion that they are hot bands, resulting from transitions originating in low lying vibrational levels of the ground electronic state.

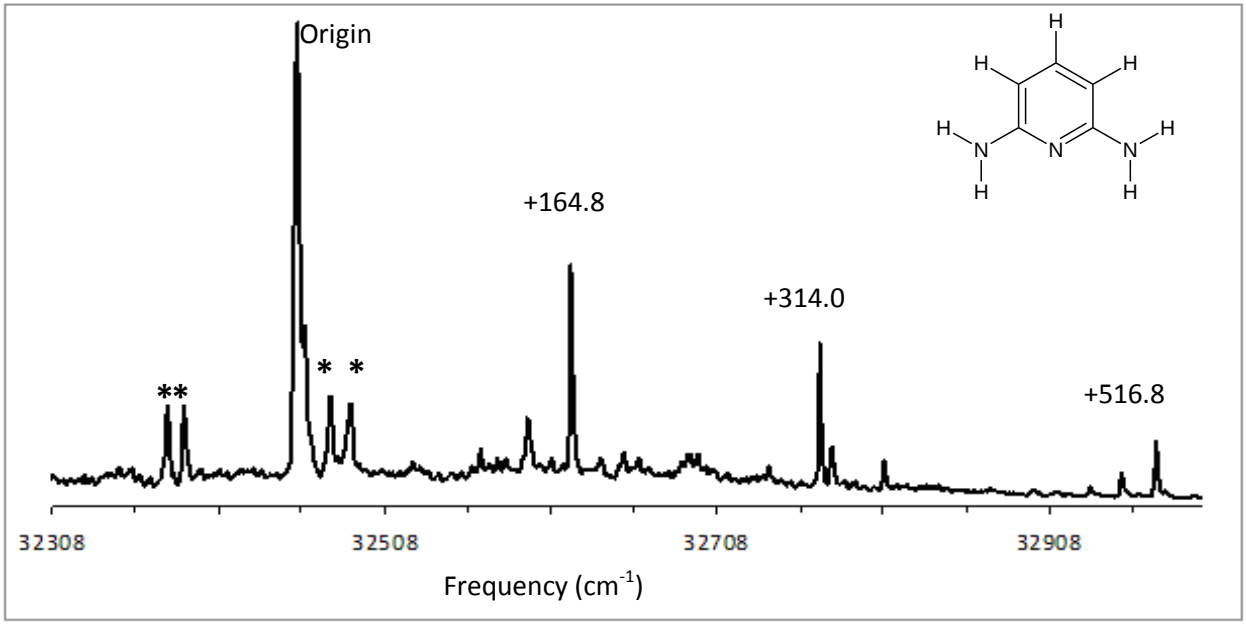

Figure 2.1: Power-normalized S1 – S0 fluorescence excitation spectrum of 26DAP at low resolution. Displacements of the prominent vibronic bands in wavenumbers relative to the origin are indicated. The peaks marked with asterisks were detectable only using a helium backing gas. The structure of 26DAP is given in the inset.

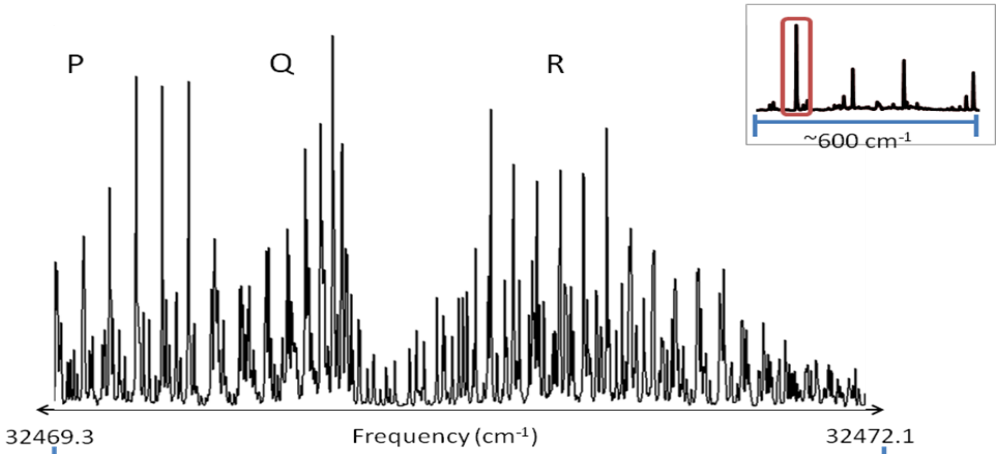

Figure 2.2: $S_1 – S_0$ Fluorescence excitation rotationally resolved spectrum of the origin band of 26DAP (see inset).

Rotationally resolved spectra of the four strongest bands in the low resolution spectrum were recorded to determine the motions that are responsible for them. Figure 2.2 shows the high resolution spectrum of the origin band of 26DAP. This spectrum exhibits a characteristic P-, Q-, and R-branch structure and spans approximately 3 cm^{-1}. It was analyzed with a rigid-rotor Hamiltonian ($H_r = A J_a^2 + B J_b^2 + C J_c^2$) for both electronic states. Initial values of the rotational constants A, B, and C required for the jb95 spectral fitting program[6] were determined using the geometry-optimized structures provided by Turbomole *ab initio* calculations (RICC2/cc-pVTZ basis set).[8] Then, the calculated spectral transitions were manually assigned to experimental transitions in the observed spectrum, and a value of the "observed minus calculated" (OMC) standard deviation was determined. Finally, optimum values of the two sets of rotational constants were found by varying them in a least-squares fashion until a minimized value of the OMC was obtained. An example of such a fit is shown in Figure 2.3. Similar procedures were used to fit the high resolution spectra of the vibronic bands at 164.8, 314.0, and 516.8 cm^{-1} above the origin.

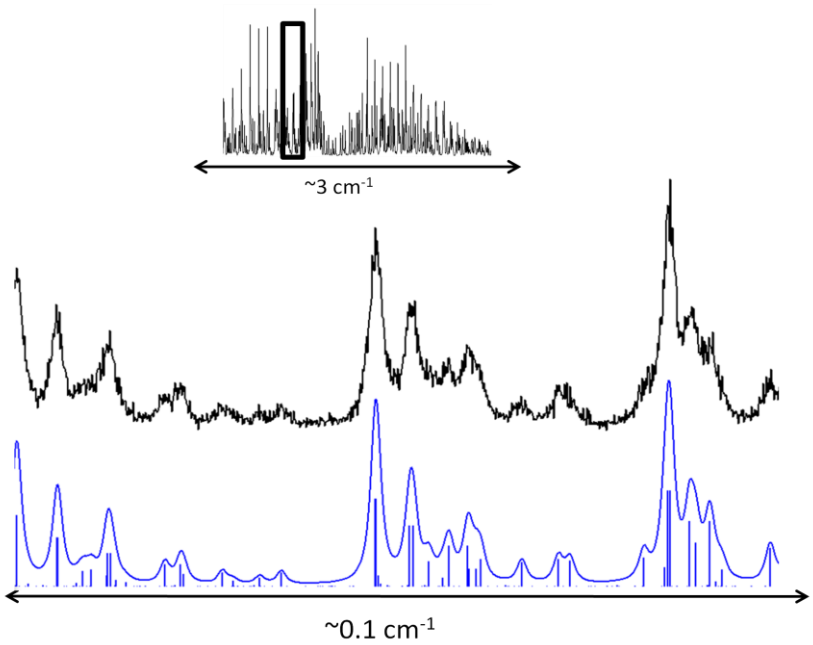

Figure 2.3: Illustration of a portion (see inset) of the fit of the origin band of 26DAP. The black trace is the experimental spectrum, the blue trace is the simulated spectrum, and the blue sticks represent calculated transitions.

All four 26DAP rotationally resolved spectra are pure *a*-type bands. Each exhibits single rovibronic linewidths of 62 MHz (FWHM). The Voigt line shape profile was fit with contributions of 20 MHz Gaussian and 42 MHz Lorentzian. The 20 MHz Gaussian component is due to Doppler broadening; its value is determined by the mutual alignment of the two beams. The 42 MHz Lorentzian component corresponds to a fluorescence lifetime of 3.1 ns for 26DAP. This lifetime falls between those of aniline (7.9 ns)[1] and 2AP (1.5 ns).[2] The 26DAP spectra were each fit with a rotational temperature of 5 K.

Table 2.1: Measured rotational constants of four bands in the S_1-S_0 electronic spectrum of 26DAP.

Parameter	S_0	Origin S_1	+164.8 S_1	+314.0 S_1	+516.8 S_1
A (MHz)	3653 (1)	3510 (1)	3497 (1)	3513 (1)	3509 (1)
B (MHz)	1988.4 (1)	2010.0 (1)	2019.2 (1)	2012.2 (1)	2008.9 (1)
C (MHz)	1290.0 (1)	1280.5 (1)	1287.5 (1)	1281.8 (1)	1282.1 (1)
ΔI (amu Å^2)	-0.77 (1)	-0.76 (1)	-2.28 (1)	-0.81 (1)	-1.43 (1)

Table 2.1 lists the inertial parameters of 26DAP that were determined in this work. The ground state rotational constants of all four vibronic bands (not shown) are the same, within experimental error. Thus, all bands originate in the same vibrational level, presumably the zero-point level (ZPL) of the S_0 state. However, the excited state rotational constants are all different, evidencing some kind of vibrational motion in the S_1 state. Unfortunately, several attempts to obtain similar data for the weaker doublet bands (marked by asterisks in Figure 2.1) were not successful.

2.5 DISCUSSION

We begin with a discussion of the structure in the electronic ground states of 26DAP and two related molecules, aniline (AN) and 2-aminopyridine (2AP), shown below (Scheme 2.1). Table 2.2 presents a comparison of the S_0 state rotational constants and inertial defects of all three molecules.[1,2]

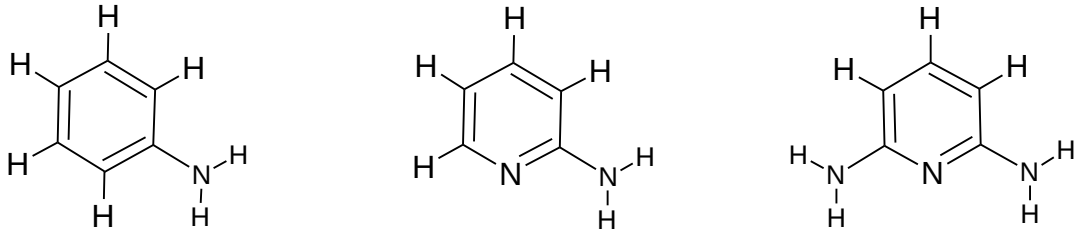

AN **2AP** **26DAP**

Scheme 2.1

Table 2.2: Comparison of the origin band rotational constants of aniline, 2AP, and 26DAP.

Parameter	Aniline (Ref. 1)	2AP (Ref. 2)	26DAP (This work)
A'' (MHz)	5617.4	5780.3	3653
B'' (MHz)	2593.8	2733.6	1988.4
C'' (MHz)	1777.0	1857.7	1290.0
ΔI'' (amu Å^2)	-0.406	-0.258	-0.77

Among the parameters listed, the inertial defects are the most instructive; $\Delta I = I_c - I_b - I_a$ is expected to be zero for a planar molecule. Aniline has ΔI = - 0.406 amu Å^2, attributable to a non-coplanar –NH_2 group distorted along the inversion coordinate.[1] 2AP has the significantly smaller value of ΔI = - 0.258 amu Å^2. Reduction in the magnitude of the inertial defect in 2AP compared to AN has been attributed to an interaction between the lone pair electrons on the ring nitrogen of 2AP with a hydrogen atom of the neighboring –NH_2 group, leading to a more planar structure.[2] But 26DAP has a larger (in magnitude) inertial defect; ΔI = - 0.77 amu Å^2. This could mean that one amino group has a similar barrier to inversion as aniline, and that the other is interacting with the lone pair electrons on the ring nitrogen, as in 2AP; or that both amino groups are distorted from planarity, in 26DAP.

Ab initio calculations using Turbomole[8] performed to explore these issues. The RICC2/cc-pVTZ level of theory[9, 10, 11] was used for both the S_0 and S_1 states. Two isomers of 26DAP were identified in the ground state calculations, one in which the two sets of amino hydrogen atoms are on the *opposite side* (OS) of the ring plane, and one in which the two sets of amino hydrogen atoms are on the *same side* (SS) of the ring plane; see below (Scheme 2.2). Of the two structures, the OS isomer has the lower energy in the ground state; $\Delta E = [E(OS) - E(SS)] = 20.8\ cm^{-1}$ according to the RICC2/cc-pVTZ calculations performed by Jordan and coworkers.[12]

OS **SS**

Scheme 2.2

Table 2.3: Comparison of the observed and calculated (RICC2/cc-pVTZ) inertial parameters of 26DAP in its ground electronic state.

Parameter	26DAP (Expt)	OS – 26DAP (Theory)	SS – 26DAP (Theory)
A'' (MHz)	3653	3682.3	3682.4
B'' (MHz)	1988.4	2001.0	2001.0
C'' (MHz)	1290.0	1299.5	1299.5
ΔI'' (amu Å^2)	-0.77	-0.902	-0.898

Table 2.3 shows a comparison of the measured rotational constants and inertial defects with the predicted ones, for both calculated structures in the ground electronic state. Unfortunately, the two sets of theoretical parameters are nearly the same, making it difficult to distinguish them. The measured parameters are quite different. The two isomers also would

be expected to exhibit slightly different nuclear spin statistical weights and transition moment orientations, but again these differences proved too small to resolve. Thus, we tentatively conclude that the observed isomer of 26DAP is the OS one because of its predicted lower energy. More information will be needed to confirm this conclusion.

The calculated values of the inertial defect, ΔI = - 0.902 (OS) and – 0.898 amu Å^2 (SS), are larger in magnitude than the observed one, ΔI = - 0.77 amu Å^2. We attribute these differences to vibrational averaging along the $-NH_2$ inversion coordinate(s). A similar phenomenon occurs in aniline[1]. Currently, it is believed that the benzene ring in aniline is flat and attached through the C-N bond to a pyramidally distorted $-NH_2$ group. The planes defined by the two groups are predicted by theory to make an angle of $\phi \sim 40°$ with respect to each other. The predicted inertial defect of this structure is - 0.498 amu Å^2, larger than the experimental value of - 0.406 amu Å^2. The two-fold barrier to inversion in ground state aniline is ~ 550 cm^{-1}. Thus, motion along this coordinate "flattens" the molecule, producing the reduced value of ΔI. Barriers significantly less than this will result in ΔI values approaching zero. This has been shown recently for the case of methyl group rotation in substituted benzenes by Morgan *et al*.[13]

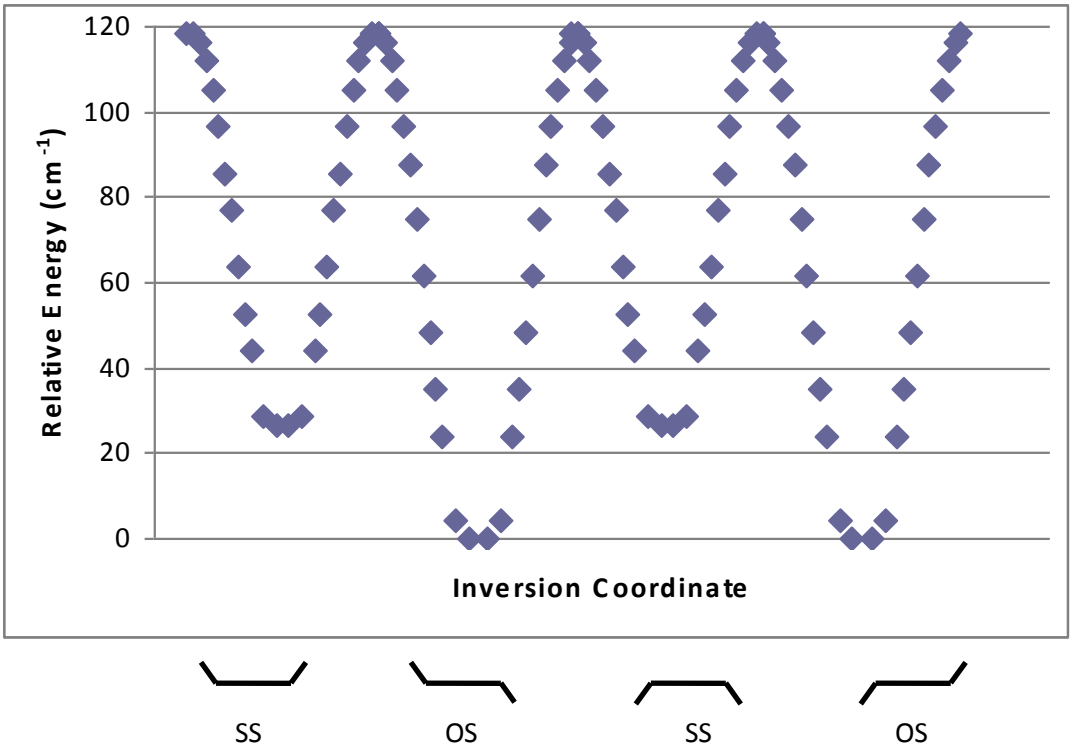

Figure 2.4: Four-fold potential energy surface for the amino-group inversion in 26DAP. The black structures shown below each well represent the orientation of the amino group hydrogens relative to the ring plane.

Figure 2.4 shows a projection of the calculated potential energy surface (PES) of 26DAP along the inversion coordinate calculated using Gaussian with the MP2/6-31G** level of theory.[14] A four-fold barrier is needed to describe this motion as there are two isomers, each with a double minimum potential. The PES shown in Fig. 4 was calculated by fixing the position of one amino group, distorting the other along its inversion coordinate in steps of 1 - 4°, and calculating the energy of the distorted structure at each step. Thus, there is a difference in energies of the four minima owing to the different energies of the two isomers, OS and SS, but the four "transition states" all have the same energy, since they are degenerate. The calculated

barriers to "inversion" of one $-NH_2$ group are of order ~ 100 cm^{-1}, where the calculated barriers to "inversion" of both $-NH_2$ groups simultaneously are of order ~ 200 cm^{-1} (*vide infra*), which seem consistent with the measured inertial defects. Significantly higher barriers oppose the interconversions of the four structures along other coordinates, such as a twisting motion around a C-NH_2 bond, which has a calculated barrier of ~ 1000 cm^{-1} in the ground state. The high barrier to amino group twisting means that perturbations due to internal rotation are unlikely to be observed.

Electronically excited 26DAP has properties that are qualitatively similar to those of the ground state, but quantitatively different. Table 2.4 presents a comparison of the S_1 state rotational constants and inertial defects of AN,[1] 2AP,[2] and 26DAP. (The rotational constants are reported here as differences between the excited state and ground state values; $\Delta A = A' - A''$, *etc.*). Notably, 26DAP has significantly smaller ΔA, ΔB, and ΔC values compared to AN and 2AP.

Table 2.4: Comparison of the differences between the excited and ground state origin band rotational constants of aniline,[1] 2AP,[2] and 26DAP.

Parameter	Aniline (Ref. 1)	2AP (Ref. 2)	26DAP (This work)
ΔA (MHz)	-330.5	-340.4	-143.0
ΔB (MHz)	40.0	38.1	21.6
ΔC (MHz)	-17.6	-20.0	-9.5
ΔI' (amu Å^2)	-0.232	-0.231	-0.76

These differences may be traced to the differences in the positions of their inertial axes, as shown in Figure 2.5. The inertial axes in AN and 2AP are almost identically oriented, with the *a* axis passing through the amino group, the *b* axis in the ring plane and close to the nitrogen-

rich end, and the *c* axis perpendicular to the ring plane. But the locations of the in-plane inertial axes are essentially switched in 26DAP owing to the increased mass of the substituents; the *a* axis is in the ring plane, closer to the nitrogen-rich end, and the *b* axis bisects the ring, passing through the ring nitrogen.

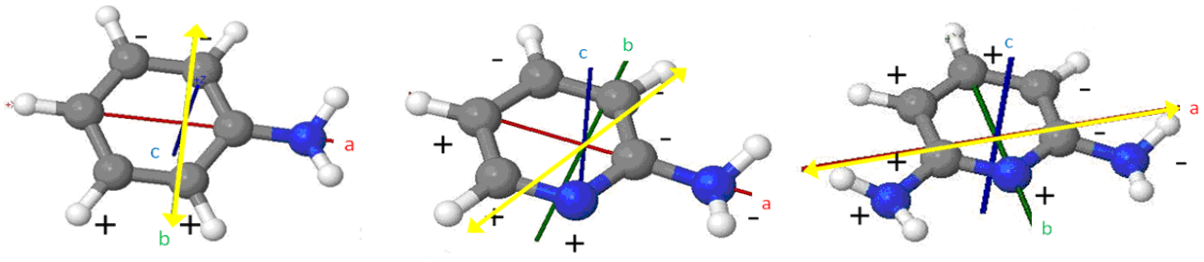

AN 2AP 26DAP

Figure 2.5: Illustration of the inertial axes, transitions moments (in yellow), and transition densities (+ and -) of aniline, 2AP, and 26DAP.

One important consequence of this "axis-switching" is an apparent change in the polarizations of the S_1-S_0 transitions in the three molecules. The electronic origin band of AN is a pure *b*-type band.[1] 2AP exhibits some *a*-type character in its origin band,[2] but 26DAP has a pure *a*-type origin band. However, as is apparent from the transition densities shown in Fig. 5, the orientations of all three S_1-S_0 transition moments in the respective *molecular* coordinate systems are essentially identical.

Table 2.5: Comparison of excited state rotational constants of four bands of 26DAP.

Parameter	Origin	+164.8 S_1	+314.0 S_1	+516.8 S_1
A' (MHz)	3510	3497	3513	3509
B' (MHz)	2010.0	2019.2	2012.2	2008.9
C' (MHz)	1280.5	1287.5	1281.8	1282.1
ΔI' (amu Å^2)	-0.76	-2.28	-0.81	-1.43

Finally, we explore the vibrational motion of 26DAP in its excited electronic state. Shown in Table 2.5 are the measured values of the excited state rotational constants and inertial defects derived from fits of the four vibronic bands; the origin band and three vibronic bands at 164.8, 314.0, and 516.8 cm^{-1} above the origin. Notably, the four sets of inertial parameters are all different, evidencing significant displacement along one or more vibrational modes. Examining the data in more detail, we see a curious trend; the changes in the magnitude of A' are not monotonic but exhibit a "zig-zag" behavior as a function of increasing energy; A' first decreases, then increases, and finally decreases again. B', C', and especially the inertial defect show the same trends. Zigzag variations of three rotational constants, and the inertial defect, as a vibration is excited are often taken as evidence for a *quasi* planar molecule and a double minimum potential energy surface along the relevant vibrational coordinate.[15, 16]

The four lowest energy calculated (CIS 6-31G**) vibrational modes of S_1 26DAP are a symmetric ring flap, an antisymmetric ring twist, an antisymmetric ring bend, and a simultaneous antisymmetric NH_2-inversion. The frequencies of these modes are 51.5, 171.7, 182.6, and 228.4 cm^{-1} in OS-26DAP, and 86.2, 176.3, 201.5, and 264.7 cm^{-1} in SS-26DAP. Of these modes, only the simultaneous antisymmetric NH_2-inversion mode (shown below in Scheme 2.3) would be expected to exhibit a double minimum potential. Previous studies have shown that modes of this type in molecules like aniline are so strongly anharmonic that it is impossible to reasonably predict their frequencies within the harmonic approximation.[17]

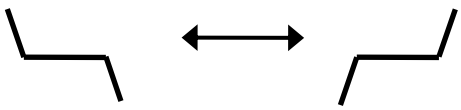

Scheme 2.3

Given this fact, the following empirical potential function was used to model the behavior of 26DAP along this coordinate in the vicinity of the presumed, lower energy OS configuration.

$$V = ks^4 - k's^2 \qquad \text{(Equation 2.1)}$$

Here, s is the displacement, the positive quartic term (with force constant *k*) creates a well, and the negative quadratic term (with force constant *k'*) raises a barrier, both at the equilibrium geometry. Potentials of this type are often successful at treating anharmonic low-frequency bending vibrations.[18] A least-squares fit of Eq. (1) to the MP2/6-31G** PES of the ground electronic state yields the values *k* = 0.00596 cm^{-1} and *k'* = 2.30 cm^{-1}, which gives the S_0 electronic state a barrier to simultaneous inversion of ~ 220 cm^{-1}. This differs from the barrier shown in Figure 2.4, because that figure only involves the inversion of a single amino group, as opposed to the simultaneous amino group inversion proposed here.

The corresponding values of these parameters in the electronically excited state were determined by treating the quartic term as a perturbation, and fitting the relative energies of the four bands in the low resolution spectrum of 26DAP using the expression:[19, 20]

$$W = W^0 + W^1 = (n + \frac{1}{2})h\nu_0 + \frac{3}{64\pi^4}(2n^2 + 2n + 1)\frac{h^2 k}{\mu^2 \nu_0^2} \qquad \text{(Equation 2.2)}$$

where $\nu_0 = \frac{1}{2\pi}\sqrt{\frac{k'}{\mu}}$. Here, W is the total energy, W^0 is the unperturbed harmonic oscillator energy from the quadratic term, and W^1 is the perturbation to the total energy produced by the quartic term. Additionally, the Franck-Condon factors of the four bands were calculated using the wavefunctions in order to fit to the relative intensities of the four bands: [19, 20]

$$\psi = \sqrt{\frac{\gamma}{\pi^{1/2} 2^n n!}} H_n[\gamma(s+s_m)] e^{[-\frac{\gamma^2}{2}(s+s_m)^2]} \pm \sqrt{\frac{\gamma}{\pi^{1/2} 2^n n!}} H_n[\gamma(s-s_m)] e^{[-\frac{\gamma^2}{2}(s-s_m)^2]} \quad \text{(Equation 2.3)}$$

where $\gamma = \sqrt{\frac{\sqrt{4\mu k'}}{\hbar}}$ and $s_m = \sqrt{\frac{k'}{2k}}$. "Best-fit" values of the parameters for excited state 26DAP were found to be μ = 3.20 amu, k = 0.0048 cm^{-1}, and k' = 2.80 cm^{-1}, which gives the S_1 electronic state a barrier to simultaneous inversion of ~ 400 cm^{-1}. These results are summarized in Table 2.6.

Table 2.6: Comparison of experimental relative vibrational energy level values to calculated results (using Eq. (2) with parameters μ = 3.20 amu, S_0 k = 0.00596 cm^{-1}, S_0 k' = 2.30 cm^{-1}, S_1 k = 0.0048 cm^{-1}, and S_1 k' = 2.80 cm^{-1}) and overlap between the ground n=0 vibrational state and the upper vibrational state defined by the quantum number (QN) listed in the table.

Vibrational QN	Experimental (cm^{-1})	Calculated (cm^{-1})	Difference (cm^{-1})	Overlap
0	0	0	0	0.89
1	164.8	149.2	15.6	0.41
2	314.0	325.7	-11.7	0.16
3	516.8	529.4	-12.6	0.06

A comparison of the PES's calculated here for 26DAP to those previously found for aniline and 2AP shows an interesting trend in the value of the barrier to amino group inversion. Previously,[21] the barrier to inversion was calculated to be 542 cm^{-1} for aniline and 353 cm^{-1} for 2AP, both found using the MP2/6-311G(2df,p) level of theory. The potential energy surface calculated here, using the MP2/6-31G(d,p) level of theory, shows a barrier to simultaneous NH_2 inversion of ~ 220 cm^{-1} in OS 26DAP. This shows that as more nitrogens are added to the ring,

the barriers to inversion decrease, in the ground electronic state. In contrast, the barriers to inversion in the S_1 electronic states increase across the series AN, 2AP, and 26DAP, rising to ~ 400 cm^{-1} in OS 26DAP. We suggest that the reason for this increase is the quinoidal form of aniline and its derivatives in the electronically excited state.[1, 22] In aniline itself, the $–NH_2$ group is attached to a position that is one bond removed from the incipient double bond, but in 2AP and 26DAP, the $-NH_2$ group is adjacent to this bond. As in the case of methyl rotors,[23] the barriers to inversion of $–NH_2$ groups are likely to depend significantly on the difference in the π-bond characters of the adjacent bonds. This apparent correlation between the number and position of nitrogen-containing substituents may have important biological relevance.

2.6 CONCLUSION

Rotationally and vibrationally resolved fluorescence excitation spectroscopy experiments on 2,6-diaminopyridine (26DAP) reveal that it exhibits a double minimum excited state potential energy surface along the amino group inversion mode, which becomes a four-fold barrier problem when the existence of two nearly degenerate “opposite-side” (OS) and “same-side” (SS) isomers is taken into account. An approximate treatment of this problem shows that OS-26DAP is the more stable isomer, and that the calculated ground state barrier to the simultaneous inversion of the two $–NH_2$ groups is substantially smaller than those of the two related molecules, aniline and 2-aminopyridine, in the ground state, but substantially larger than those of the same molecules in their electronically excited states. In the next chapter, a study of another nitrogen containing molecule, Pyrrolidinobenzonitrile (PYRBN), will be presented.

2.7 ACKNOWLEDGEMENTS

I wish to thank Justin W. Young with experimental assistance, and Dr. Ken Jordan, Dr. Wissam Al-Saidi, Dr. Daniel Schofield, and Xiaoge Su for their assistance with the theoretical calculations. Funding from NSF Grant # CHE-0911117 also is acknowledged. This work is published in J. Phys. Chem. A **2010** *114* (45), 12005-12009.

2.8 REFERENCES

1. Sinclair, W. E.; Pratt, D. W. *J. Chem. Phys.* **1996**, *105*, 7942.

2. Borst, D. R.; Roscioli, J. R.; Pratt, D. W. *J. Phys. Chem. A* **2002**, *106*, 4022.

3. Jorgensen, W. L.; Pranata, J. *J. Am. Chem. Soc.* **1990**, *112*, 2008.

4. Pranata, J.; Wierschke, S. G.; Jorgensen, W. L. *J. Am. Chem. Soc.* **1991**, *113*, 2810.

5. Majewski, W. A.; Pfanstiel, J. F.; Plusquellic D. F.; Pratt, D. W. In *Laser Techniques in Chemistry*, Meyers, A. B.; Rizzo, T. R., Eds.; John Wiley & Sons, Inc: New York, 1993.

6. Plusquellic, D. F; Suenram, R. D.; Maté, B.; Jensen J. O.; Samuels, A. C. *J. Chem. Phys.* **2001**, *115*, 3057.

7. Gerstenkorn S.; Luc, P. Atlas *du spectroscopie d'absorption de la molecule d'iode*, CNRS: Paris, 1978/1982.

8. TURBOMOLE V6.1; University of Karlsruhe and Forschungszentrum Karlsruhe GmbH, 1989-2007, TURBOMOLE GmbH, since 2007; 2009; available from http://www.turbomole.com.

9. Hättig, C. *J. Chem. Phys.* **118**, *7751*, 2003.

10. Köhn, A.; Hättig, C. *J. Chem. Phys.* **119**, *5021*, 2003.

11. Woon, D. E.; Dunning, T. H., Jr. *J. Chem. Phys.* **1995**, *103*, 4572.

12. Su, X.; Al-Saidi, W. A.; Jordan, K. D. in preparation.

13. Morgan, P. J.; Alvarez-Valtierra L.; Pratt, D. W. *J. Phys. Chem. A* **2009**, *113*, 13221.

14. Frisch M. J. *et al.*, Gaussian 03, Gaussian Inc.: Wallingford, CT, 2004.

15. Jagannathan S.; Pratt, D. W. *J. Chem. Phys.* **1994**, *100*, 1874.

16. Oka, T. *J. Mol. Struct.* **1995**, *352/353*, 225.

17. Wojciechowski, P. M.; Zierkiewicz, W.; Michalska, D.; Hobza, P. *J. Chem. Phys.* **2003**, *118*, 10900.

18. Wollrab, J. E. *Rotational Spectra and Molecular Structure.* Academic Press, Inc.: New York, 1967.

19**.** Flygare, W. H. *Molecular Structure and Dynamics.* Prentice-Hall, Inc.: Englewood Cliffs, 1978.

20**.** Pauling, L.; Wilson, E. B. *Introduction to Quantum Mechanics.* McGraw-Hill Book Company, Inc.: New York, 1935.

21. Bludsky, O.; Sponer, J.; Leszczynski, J.; Spirko, V.; Hobza, P. *J. Chem. Phys.* **1996**, *105*, 11042.

22. Cvitas, T.; Hollas, J. M.; Kirby, G. H. *Mol. Phys.* **1970**, *19*, 305.

23. Spangler L. H.; Pratt, D. W. In *Jet Spectroscopy and Molecular Dynamics*, Hollas, J. M.; Phillips, D. Eds., Chapman & Hall: New York, 1995.

3.0 ROTATIONALLY RESOLVED $S_1 - S_0$ ELECTRONIC SPECTRA OF PYRROLIDINOBENZONITRILE

3.1 ABSTRACT

Pyrrolidinobenzonitrile (PYRBN), a derivative of 4,4'-dimethylaminobenzonitrile (DMABN), has been examined here using high resolution fluorescence excitation spectroscopy in the presence of an electric field varying from 0 – 846 V/cm. The *b*-type origin band reveals that the transition moment is along the short, in plane axis of the molecule. Upon excitation the inertial defect remains unchanged, which suggests that the molecule's planarity remains constant. The dipole moment is found to increase from 8.06 to 10.45 D upon electronic excitation. Taken together, these data show that the first excited electronic state of PYRBN is a locally excited ^1L_b state with little charge transfer character.

3.2 INTRODUCTION

Recently, it was discovered that electronic excitation of the molecule 1-phenylpyrrole (1PP, see Figure 3.1 (A)) to its first excited state results in a reversal of the direction of its permanent electric dipole moment.[1] The 1PP dipole moment points towards the pyrrole ring in the ground electronic state (S_0), but towards the benzene ring in the excited S_1 state. In this report, we examine whether or not this same phenomenon occurs in the related molecule pyrrolidinobenzonitrile (PYRBN, see Figure 3.1 (B)).

1PP[2] and PYRBN[3] are of interest because they are capable of undergoing twisted intermolecular charge transfer (TICT) upon electronic excitation. The idea of TICT and dual fluorescence was introduced by Lippert and coworkers' study of DMABN,[4] and the subsequent study of Grabowski and coworkers on related model compounds.[5] DMABN and related molecules have been found to exhibit dual fluorescence in solution.[6] The two types of fluorescence that can be found include a normal *b*-type fluorescence that can be assigned to an S_1 - S_0 transition from a locally excited state, and a red-shifted *a*-type fluorescence that is believed to be from a TICT state that is stabilized by polar solvent. As a result, the TICT state is presumed to possess a large degree of charge separation associated with a twisted arrangement of two chromophores.

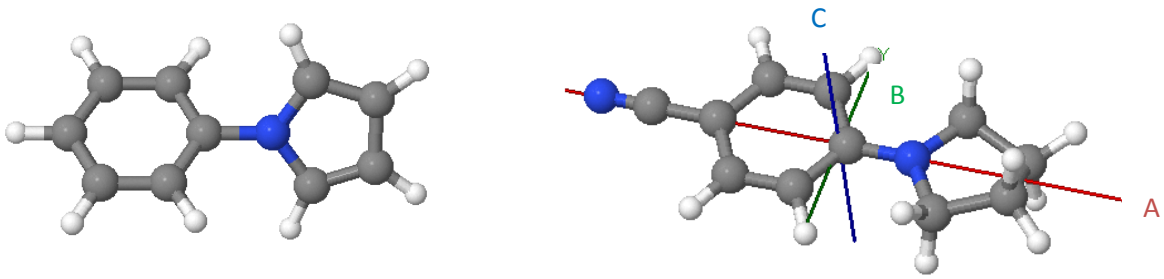

(A) 1PP (B) PYRBN

Figure 3.1: Structure of 1PP (A) and PYRBN (B) with labeled inertial axes.

Previous studies on PYRBN include solution, polymer matrix, and gas phase fluorescence experiments. Both solution phase[7] and polymer matrix[8] studies have demonstrated the dual fluorescence of PYRBN. Gas phase studies performed by Walters[9-12] and Zimmerman[13] have found fluorescence from only the L_b band for PYRBN, but saw both L_a and L_b fluorescence for

ester derivatives of DMABN. They were able to obtain approximate rotational constants of all species using contour fits.

In this work, high resolution gas phase spectra of PYRBN were recorded at varying external electric field strengths. This study has confirmed that the origin band of PYRBN involves a localized L_b state (using Platt's notation),[14] and that no change in planarity occurs upon excitation to that state, as seen by the unchanged inertial defect in the 100% *b*-type band. The dipole moment increases in magnitude, but does not change direction upon electronic excitation, which is in contrast to the observed behavior of 1PP.

3.3 EXPERIMENTAL

PYRBN was purchased from Maybridge and used without further purification. Rotationally resolved electronic spectra were observed using the CW molecular beam spectrometer described in detail elsewhere.[15] Briefly, approximately 1 g of PYRBN was heated in a quartz reservoir to around 180 °C (which is slightly below its melting point), seeded into argon backing gas at ~ 500 torr, and expanded through a ~ 200 µm nozzle. The expansion was skimmed 2 cm downstream by a 1 mm skimmer and probed with the laser 15 cm downstream from the nozzle. The excitation source was an Ar^+-pumped CW, single-frequency tunable ring dye laser externally doubled by a Spectra-Physics Wavetrain using a 625 nm BBO crystal, yielding ~ 100 µW of power in the UV. The single rovibronic level linewidths were minimized by aligning the molecular beam and laser beam at right angles. The fluorescence was collected using spatially selective optics and detected by a PMT (EMI 9813QB). The data collected were processed using jba95 data acquisition software.[16] Absolute frequencies were determined by comparison to the

iodine absorption spectrum[17] which was simultaneously recorded, providing an absolute frequency accuracy of +/- 30 MHz. Relative frequencies were determined using frequency markers that were created by passing a small portion of the fundamental through a stabilized etalon with a free spectral range of 299.7520 ± 0.0005 MHz and are accurate to 1 MHz or less. To obtain the Stark spectra, a set of wire mesh plates was positioned approximately 0.5 cm above and below the intersection of the laser and molecular beams and a voltage was applied across them. The spectra were recorded by collecting the fluorescence in the presence of electric fields of various strengths. The plate separation was calibrated using the known dipole moments of aniline.[18]

3.4 RESULTS

Figure 3.2 (A) shows the zero-field high resolution electronic spectrum of the origin band of PYRBN. This spectrum exhibits the characteristic P-, Q-, and R-branch structure of a *b*-type transition and spans approximately 3 cm^{-1}. It was analyzed with a rigid-rotor Hamiltonian ($H_r = A J_a^2 + B J_b^2 + C J_c^2$) for both electronic states. Initial values of the rotational constants A, B, and C required for the jb95 spectral fitting program[16] were determined using the geometry-optimized structures provided by Gaussian *ab initio* calculations (M052X 6-31G** basis set).[19] Then, the calculated spectral transitions were manually assigned to experimental transitions in the observed spectrum, and a value of the "observed minus calculated" (OMC) standard deviation was determined. Finally, optimum values of the two sets of rotational constants were found by varying them in a least-squares fashion until a minimized value of the OMC was obtained. An example of the zero-field fit is shown in Figure 3.2 (B).

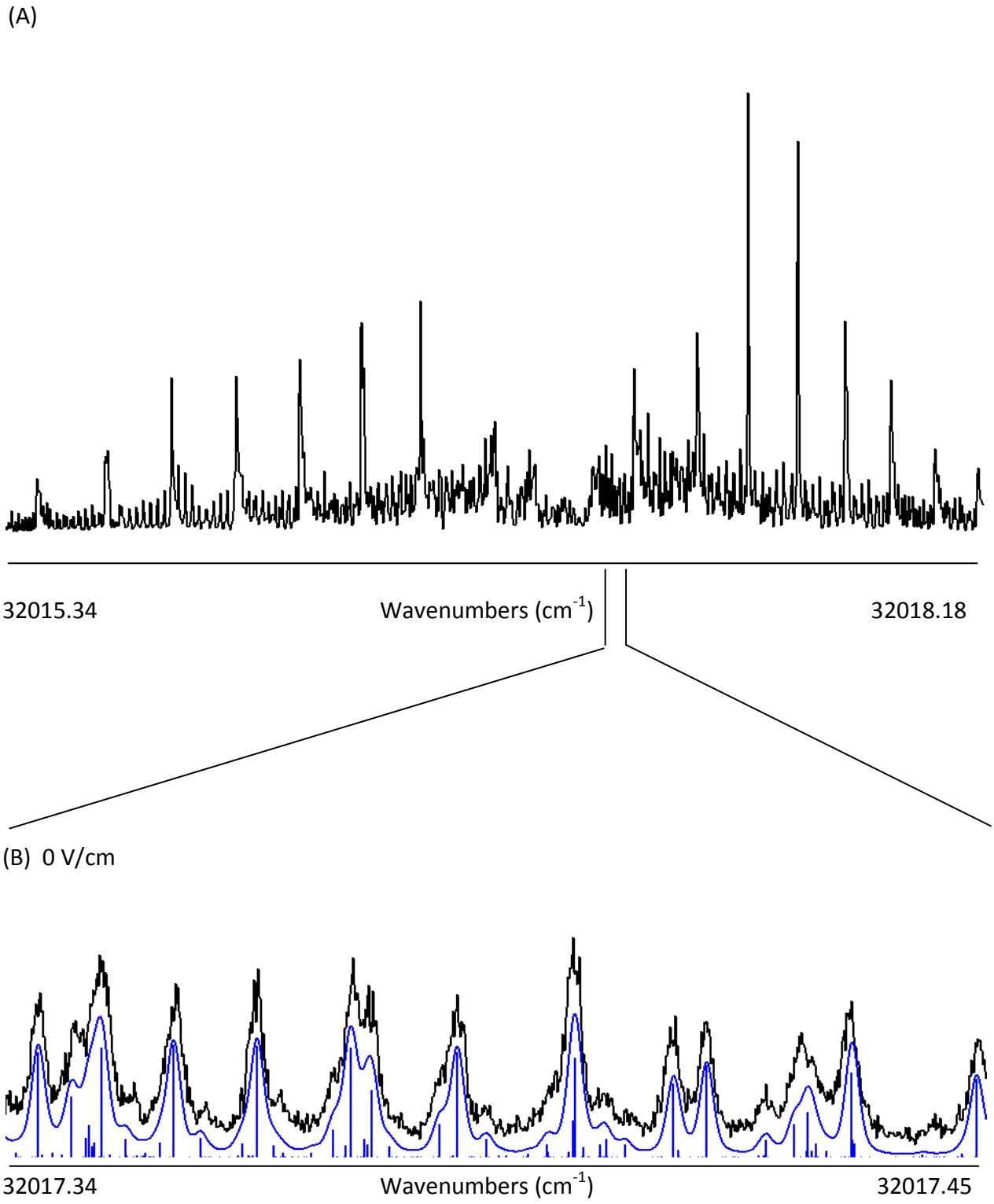

Figure 3.2: (A) Rotationally resolved electronic spectrum of PYRBN origin band. (B) Expansion of a portion of the origin band with no applied external electric field.

The spectrum of the PYRBN origin band shown in Figure 3.2 is 100% *b*-type with single rovibronic linewidths of 50 MHz (FWHM). The Voigt line shape profile was fit with contributions of 22 MHz Gaussian and 30 MHz Lorentzian. The 22 MHz Gaussian component is due to Doppler broadening; its value is determined by the mutual alignment of the two beams. The 30 MHz Lorentzian component corresponds to a fluorescence lifetime of 5.3 ns. The spectrum was fit with a rotational temperature of 5 K. Table 3.1 contains the rotational constants of the PYRBN origin band determined from experiment. The ground state rotational constants are similar to those previously reported by Walters and coworkers,[20] but there is a noticeable difference due to the fact that a contour fit was used by Walters, which does not allow the determination of precise rotational constants.

Figure 3.3 (A) – (C) show fits to the experimental spectra of PYRBN at increasing electric field strengths. In order to fit the Stark spectra, a perturbed Hamiltonian is needed ($H = H_r + H_e$ where $H_e = -E_z \Sigma \mu_g \Phi_{zg}$ where g=a,b,c). As the electric field strength increases, the electronic transitions split. For a *b*-type transition, the Stark effect is linear for levels connected by μ_a and μ_c, and quadratic for levels connected by μ_b. For PYRBN, we find that only one component of μ is non-zero, μ_a. Its value in both electronic states is listed in Table 3.1.

(A) 84.6 V/cm

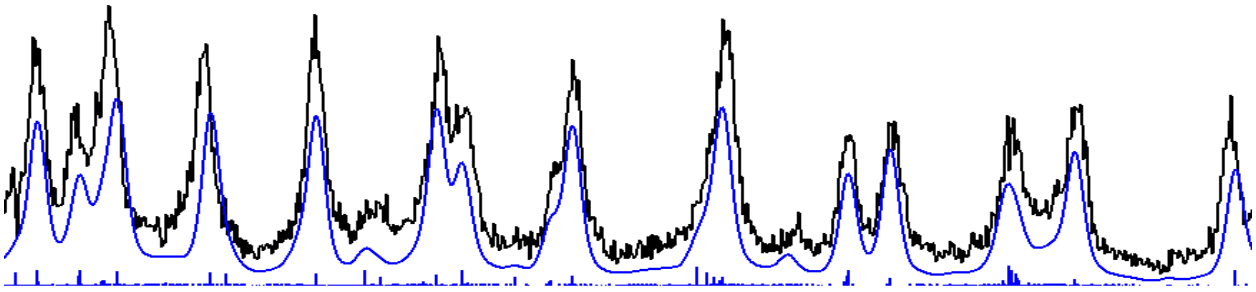

(B) 422 V/cm

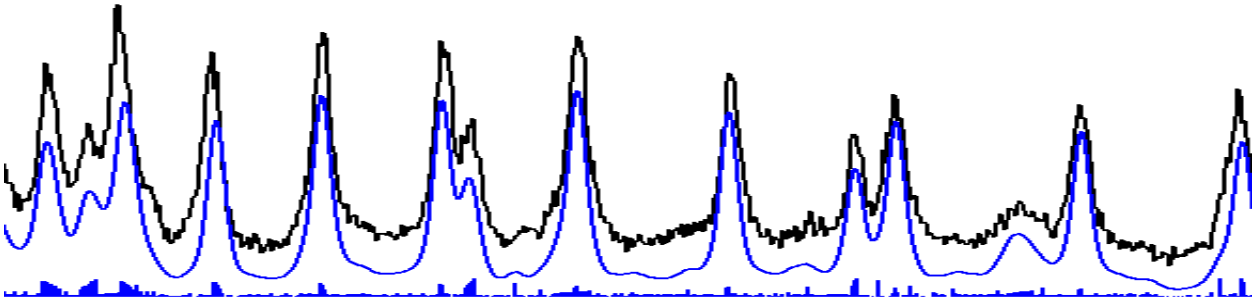

(C) 846 V/cm

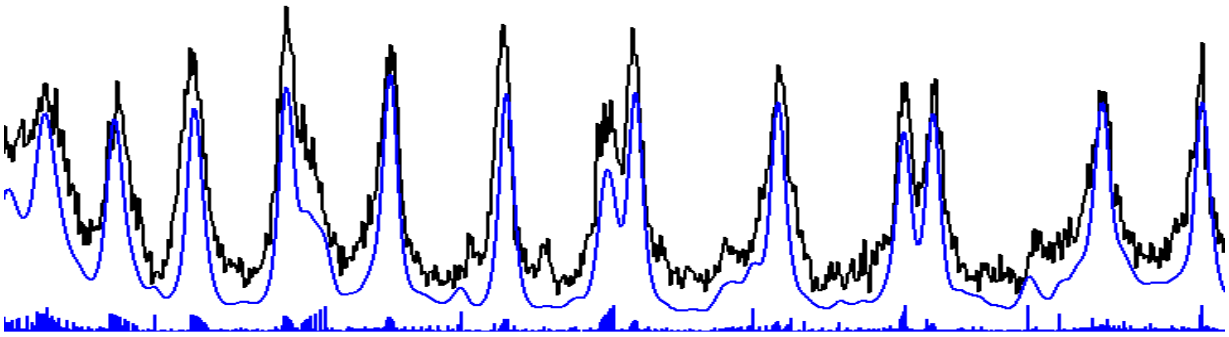

32017.34 Wavenumbers (cm^{-1}) 32017.45

Figure 3.3: (A) – (C) Rotationally resolved electronic spectrum of PYRBN origin band expansion with increasing external electric field strength.

Table 3.1: PYRBN origin band experimental inertial parameters and dipole moments.[20]

Parameter	S_0 experimental	S_1 experimental	S_0 Walters[a]
A (MHz)	3083 (1)	3006 (1)	3075
B (MHz)	366.2 (1)	367.2 (1)	352.9
C (MHz)	331.8 (1)	331.7 (1)	319.0
ΔI (amu Å^2)	-20.67 (7)	-20.68 (7)	-12.26
μ_a (Debye)	8.06 (1)	10.45 (1)	NA

[a] Howells, et al. (Ref. 20)

3.5 DISCUSSION

Table 3.2 lists the measured rotational constants of the PYRBN origin band, as well as the calculated ground state and excited state parameters obtained using *ab initio* methods.[19] The S_2 state was calculated using the root=2 command. To the level of theory used here, the theoretical inertial parameters and dipole moments were the same for both the S_1 and S_2 states.

Table 3.2: PYRBN origin band experimental and calculated inertial parameters.

Parameter	S_0 exp.	S_0 calculated (M052X/6-31G**)	S_1 exp.	S_1 calculated (CIS/6-31G**)	S_2 calculated (CIS/6-31G**)
A (MHz)	3083 (1)	3100.73 (0.57%)	3006 (1)	3039.10 (1.10%)	3039.10 (1.10%)
B (MHz)	366.2 (1)	367.35 (0.31%)	367.2 (1)	366.93 (0.07%)	366.93 (0.07%)
C (MHz)	331.8 (1)	332.87 (0.32%)	331.7 (1)	333.32 (0.45%)	333.32 (0.45%)
ΔI (amu Å^2)	-20.67 (7)	-20.49 (0.87%)	-20.68 (7)	-27.42 (28.0%)	-27.42 (28.0%)
μ_a (Debye)	8.06 (1)	8.113 (0.66%)	10.45 (1)	9.620 (8.27%)	9.620 (8.27%)

The M052X/6-31G** theoretical rotational constants of the ground state match up well with the experimental ones, with errors of less than 1%. The calculated and measured inertial defects also are in good agreement. The value of the inertial defect, -20.67 amu Å ^{2}, is mainly due to the out of plane character of the five-membered pyrrolidine ring, because the benzonitrile portion of the molecule is planar, according to the theortical calculations. See Figure 3.4. The $-CH_2$ groups in the saturated ring are displaced above and below the aromatic ring by ±13 Å.

There are a few interesting trends among the excited state inertial parameters listed in Table 3.2. First, the A rotational constants decreases upon excitation, but the B and C rotational constants remain relatively the same. This shows that the molecule spreads out in the direction perpendicular to *a* when the photon is absorbed (See Fig. 1). The CIS/6-31G** calculations reproduce these trends. However, theory predicts a significantly increased value of the inertial defect, whereas experiment shows the value of ΔI to be essentially the same in both electronic states. The degree of non-planarity of the molecule does not change upon excitation by light.

Using theory, we can explore many additional interesting properties of PYRBN. The lowest energy excited electronic state (S_1) calculated by Gaussian CIS/6-31G** is the L_a state (using Platt's notation),[14] and the second excited electronic state (S_2) is calculated to be the L_b state. The calculated molecular orbitals, transition densities, and transition moments are shown in Figure 3.5. The calculated S_1 state has 66% HOMO – LUMO character and is shown in

Figure 3.5 (A). The calculated S_2 state has 60% HOMO – LUMO+1 character and is shown in Figure 3.5 (B).

(A) S_0

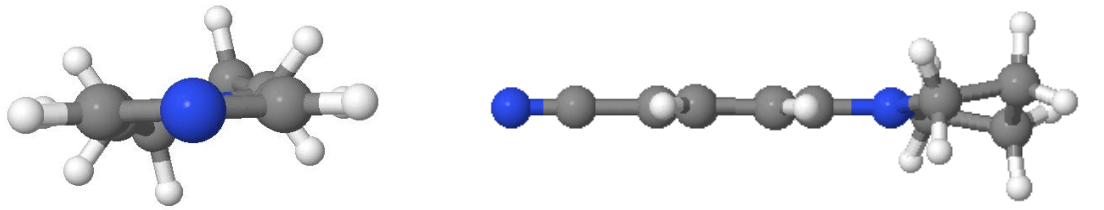

(B) S_1

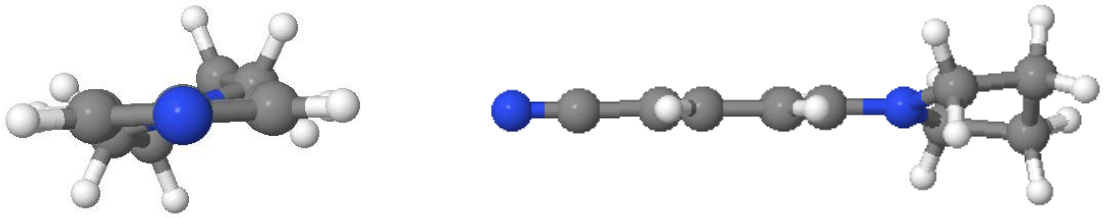

Figure 3.4: Calculated structure of PYRBN (A) ground state using M052X/6-31G and (B) excited state using CIS/6-31G**.**

Previous studies[6] using CNDO/s calculations have shown that in aminobenzonitriles the L_b state is lower in energy than the L_a state, which implies that the order of the two lowest energy excited electronic levels should be the reverse of that which was calculated here. This is supported by experiment; the origin band of PYRBN is a pure *b*-type band, showing unambiguiosly that the S_1 state is ^1L_b, not ^1L_a. In previous studies,[21] including only single excitations has been found to be inadequate for highly symmetric aromatic molecules with considerable near-degeneracy in their π–electron systems. Roos, et al.[22] concluded that the CIS method will not even be capable of giving a qualitatively correct description of excited state levels, owing to its neglect of electron correlation. To address this problem, our collaborators

in the Jordan Group at the University of Pittsburgh ran RICC2/cc-pVTZ[23-26] calculations to determine the shapes of the molecular orbitals in PYRBN. They found that the RICC2-calculated LUMO is equivalent to the LUMO+1 of the CIS calculations, and that the RICC2-calculated LUMO+1 is equivalent to the LUMO of the CIS calculations. From their results, they predict the S_1 state to be L_b and the S_2 state to be L_a, which agrees with the experimental observations.

Table 3.2 also includes information on the experimental and calculated dipole moment. A previous study[27] found a dipole moment of μ_a = 17.0 D for the L_b state in dioxane solution using solvatochromic methods. This is larger than the experimentally determined values presented here. The direction of the dipole moment cannot be determined by this experiment, but a reasonable assignment can be made based on calculations and chemical intuition. The experiment does show that the direction of the dipole moment does not change and that the magnitude of the dipole moment increases upon excitation. Based on calculations and the fact that the nitrile moiety is an accepting group, it can be assumed that the dipole moment points toward the nitrile group in both the group and excited electronic states. Upon excitation the magnitude of the dipole moment increases by 2.39 D, which is a 25% change. This change in magnitude can be visualized by the density difference MO in Figure 3.5 where areas of electronic density gain are balanced by areas of electronic density loss.

(A) Calculated S_1 HOMO-LUMO (66%)

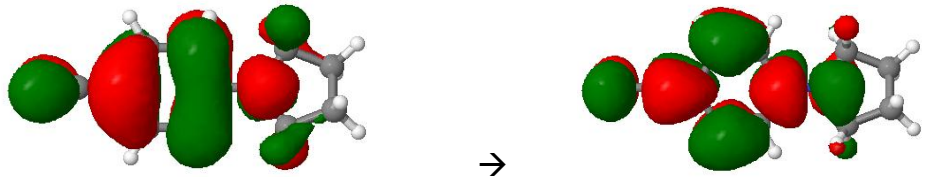

Transition Density Diagram Density Difference MO

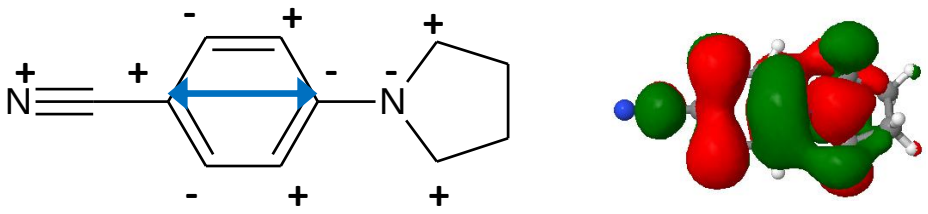

(B) Calculated S_2 (60%) HOMO-LUMO+1

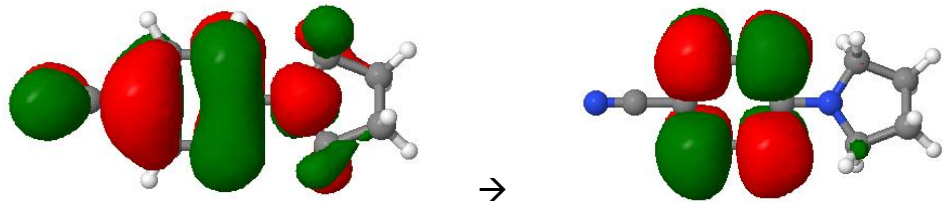

Transition Density Diagram Density Difference MO

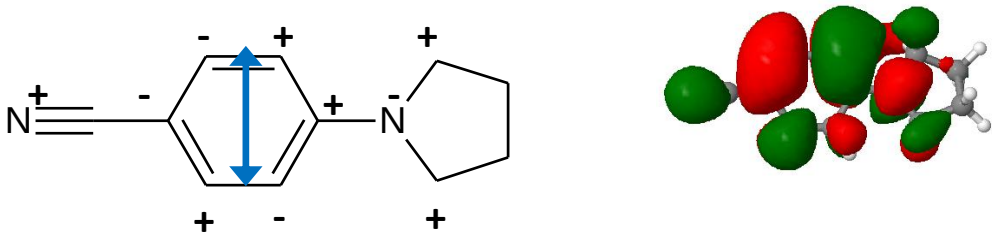

Figure 3.5: Molecular orbitals, transition densities, and transition moments using Gaussian CIS 6-31G of (A) the calculated S_1 state and (B) the calculated S_2 state. Green represents electronic gain, and red represents electronic loss. The RICC2 cc-pVTZ results switch the LUMO and LUMO+1 molecular orbitals.**

Using the fact that moving one electron one angstrom results in a charge displacement of 4.8 D (1 e^- · Å = 4.8 D), the experimental $\Delta\mu(S_1\text{-}S_0)$ ~ 2.39 D and the 4.2 Å calculated distance between the centers of the two rings suggests that a transfer of 0.13 e^- occurs upon excitation. Using the coulomb potential equation, that charge transfer leads to a stabilization of ~ 432 cm^{-1}. This is significantly less than the stabilization found experimentally in glycerol triacetate solution (7780 cm^{-1})[28] and in a polymer matrix of poly(vinyl alcohol) (5760 cm^{-1}).[29] The decrease in stabilization from solution phase to polymer matrix to gas phase could be due to the decreased presence of polar molecules that can interact with the electron density of PYRBN as one goes from solution phase to polymer matrix, and the complete lack of polar molecules available for interaction in the gas phase.

A molecule that is similar to PYRBN which was recently studied by our group is 1-phenylpyrrole (1PP).[1] The structure of 1PP is shown in Figure 1 (A), and PYRBN is shown in Figure 1 (B). Structurally, 1PP and PYRBN are similar except that PYRBN has a nitrile group in the *para* position of the benzene ring, and it has a saturated pyrrolidine group instead of an aromatic pyrrole group.

There are many spectroscopic similarities between PYRBN and 1PP. The transition moment is located along the short axis of the benzene plane in both PYRBN and 1PP. The transition is purely *b*-type in PYRBN, but a mixed *b/c*-type in 1PP due to a twist between the ring planes. Both the PYRBN origin band and the vibronic bands of 1PP that were studied are mainly *b*-type, which does not correspond to the TICT state, which would instead be *a*-type.[6]

In 1PP, the ground state dipole moment points toward the pyrrole ring, but in the excited state it reverses direction and points toward the benzene ring with a change in magnitude of around 2.5 D, from -1.5 D in the ground state to 1.0 D in the excited state. This differs from PYRBN, where the dipole moment points toward the nitrile group from the benzene ring in both the ground and excited electronic states. This is likely due to the presence of the nitrile accepting group in PYRBN, which would favor increased electron density toward the nitrile end of the molecule. The magnitude of the dipole moment is much larger in PYRBN than in 1PP, but upon excitation the magnitude of the dipole moment change is similar in both molecules.

Upon excitation, a transfer of 0.13 e^- occurs in PYRBN compared to 0.15 e^- in 1PP.[1] That charge transfer leads to a stabilization of ~ 432 cm^{-1} in PYRBN and ~ 700 cm^{-1} in 1PP. There is a slight difference in the distance between the center of the rings in the two molecules, with a distance of 4.2 Å in PYRBN and 3.6 Å in 1PP. The slightly larger distance in PYRBN leads to a smaller stabilization than that in 1PP, but both molecules are significantly stabilized by the charge transfer.

Another interesting comparison between PYRBN and 1PP is in the change of the magnitude of their inertial defects upon electronic excitation. PYRBN has no change in its inertial defect upon excitation, but in the 1PP vibronic bands studied the magnitude of the inertial defect decreases by ~15 amu $Å^2$ upon excitation. That shows that 1PP is becoming significantly more planar upon excitation, but PYRBN does not have a measurable change in its planarity. This could be due to the presence of the nitrile group, or more likely due to the non-

aromaticity of the pyrrolidine ring in PYRBN as opposed to the aromatic pyrrole ring found in 1PP.

3.6 CONCLUSIONS

The molecule PYRBN has been examined here using high resolution fluorescence excitation spectroscopy in the presence of an electric field varying from 0 – 846 V/cm. The *b*-type fluorescence band reveals that the transition moment is along the short, in plane axis of the molecule, and shows that the S_1 state is an ^1L_b state. Upon excitation the inertial defect remains unchanged, which suggests that the degree of non-planarity in PYRBN remains constant. The dipole moment is found to increase from 8.06 to 10.45 D upon electronic excitation. All of these facts point to significant charge reorganization in PYRBN upon excitation by light, but these changes are not sufficient to significantly change the character of the S_1 state.

3.7 ACKNOWLEDGEMENTS

I wish to thank Adam J. Fleisher for experimental assistance, and Ken Jordan, Dr. Wissam Al-Saidi, Dr. Daniel Schofield, and Xiaoge Su for their assistance with the theoretical calculations. Funding from NSF Grant # CHE-0911117 also is acknowledged.

3.8 REFERENCES

1. J. A. Thomas, J. W. Young, A. J. Fleisher, L. Alverez-Valtierra, and D. W. Pratt, J. Phys. Chem. Lett. **2010**, *1*, 2017-2019.

2. K. Okuyama, Y. Numata, S. Odawara, I. Suzuka, J. Chem. Phys. **1998**, *109*, 7185-7196.

3. B. D. Howells, M. T. Martinez, T. F. Palmer, J. P. Simons, and A. Walters, J. Chem. Soc. Faraday Trans. **1990**, 86 (11*)*, 1949-1956.

4. E. Lippert, W. Luder, H. Boos, in Advances in Molecular Spectroscopy, A. Mangini, Ed., Pergamon, 1962, Oxford, p 443.

5. K. Rotkiewicz, K. H. Grellmann, Z. R. Grabowski, Chem. Phys. Lett. **1973**, *19*, 315.

6. W. Rettig and V. Bonačić-Koutecký, Chem. Phys. Lett. **1979**, *62 (1)*, 115-120.

7. K. Dahl, R. Biswas, N. Ito, and M. Maroncelli, J. Phys. Chem. B **2005,** *109,* 1563-1585

8. K. A. Al-Hassan and W. Rettig, Chem. Phys. Lett. **1986**, *126*, 273.

9. B. D. Howells, M. T. Martinez, T. F. Palmer, J. P. Simons, and A. Walters, J. Chem. Soc. Faraday Trans. **1990**, *86(11)*, 1949-1956.

10. B. D. Howells, J. McCombie, T. F. Palmer, J. P. Simons, A. Walters, J. Chem. Soc. Faraday Trans. **1920**, *88(18)*, 2587-2594.

11. B. D. Howells, J. McCombie, T. F. Palmer, J. P. Simons, A. Walters, J. Chem. Soc. Faraday Trans. **1920**, *88(18)*, 2595-2601.

12. B. D. Howells, J. McCombie, T. F. Palmer, J. P. Simons, A. Walters, J. Chem. Soc. Faraday Trans. **1920**, *88(18)*, 2603-2610.

13. C. Dedonder-Lardeux, C. Jouvet, S. Martrenchard, D. Solgadi, J. McCombie, B. D. Howells, T. F. Palmer, A. Subaric-Leitis, C. Monte, W. Rettig, and P. Zimmermann, Chem. Phys. **1995**, *191*, 271-287.

14. J. R. Platt, J. Chem. Phys. **1949**, *17 (5)*, 484.

15. W. A. Majewski, J. F. Pfanstiel, D. F. Plusquellic and D. W. Pratt, in Laser Techniques in Chemistry, A. B. Meyers and T.R. Rizzo, Eds., John Wiley & Sons, Inc. 1993, New York.

16. D. F Plusquellic, R. D. Suenram, B. Maté, J. O. Jensen and A. C. Samuels, J. Chem. Phys. **2001**, *115*, 3057.

17. S. Gerstenkorn and P. Luc, Atlas *du spectroscopie d'absorption de la molecule d'iode*, CNRS, Paris, 1978/1982.

18. T. M. Korter, D. R. Borst, C. J. Butler, and D. W. Pratt, J. Am. Chem. Soc. **2001**,

123, 96-99.

19. M. J. Frisch et al., Gaussian 03, Gaussian Inc., Wallingford, CT (2004).

20. B. D. Howells, M. T. Martinez, T. F. Palmer, J. P. Simons, and A. Walters, J. Chem. Soc. Faraday Trans. **1990**, *86(11)*, 1949-1956.

21. J. W. Ribblett, D. R. Borst, and D. W. Pratt, J. Chem. Phys. **1999**, *111(18)*, 8454.

22. B. O. Roos, K. Andersson, and M. P. Fülscher, Chem. Phys. Lett. **1992**, *192(1)*, 5-12.

23. TURBOMOLE V6.1 2009, a development of University of Karlsruhe and Forschungszentrum Karlsruhe GmbH, 1989-2007, TURBOMOLE GmbH, since 2007; available from http://www.turbomole.com.

24. Hättig, C. *J. Chem. Phys.* **118**, *7751*, 2003.

25. Köhn, A.; Hättig,C. *J. Chem. Phys.* **119**, *5021*, 2003.

26. Woon, D. E.; Dunning, Jr., T. H. *J. Chem. Phys.* **1995**, *103*, 4572-4585.

27. W. Baumann, H. Bischof, J.-C. Fröhling, C. Brittinger, W. Rettig, and K. Rotkiewicz, J. Photochem. Photobiol. A. Chem. **1992**, *64*, 49-72.

28. D. Braun, P. L. Nordio, A. Polimeno, and G. Saielli, J. Chem. Phys. **1996**, *208*, 127-136.

29. K. A. Al-Hassan, and T. Azumi, Chem. Phys. Lett. **1988**, *146*, 121-124.